Environmental Science & Technology

pubs.acs.org/est

Article

Closing Dichloramine Decomposition Nitrogen and Oxygen Mass Balances: Relative Importance of End-Products from the Reactive Nitrogen Species Pathway

Huong T. Pham, David G. Wahman, and Julian L. Fairey*

Cite This: *Environ. Sci. Technol.* 2024, 58, 2048−2057

Read Online

ACCESS | Metrics & More | Article Recommendations | Supporting Information

ABSTRACT: In drinking water chloramination, monochloramine autodecomposition occurs in the presence of excess free ammonia through dichloramine, the decay of which was implicated in *N*-nitrosodimethylamine (NDMA) formation by (i) dichloramine hydrolysis to nitroxyl which reacts with itself to nitrous oxide (N_2O), (ii) nitroxyl reaction with dissolved oxygen (DO) to peroxynitrite or mono/dichloramine to nitrogen gas (N_2), and (iii) peroxynitrite reaction with total dimethylamine (TOTDMA) to NDMA or decomposition to nitrite/nitrate. Here, the yields of nitrogen and oxygen-containing end-products were quantified at pH 9 from $NHCl_2$ decomposition at 200, 400, or 800 μeq $Cl_2 \cdot L^{-1}$ with and without 10 μM-N TOTDMA under ambient DO (~500 μM-O) and, to limit peroxynitrite formation, low DO (≤40 μM-O). Without TOTDMA, the sum of free ammonia, monochloramine, dichloramine, N_2, N_2O, nitrite, and nitrate indicated nitrogen recoveries ±95% confidence intervals were not significantly different under ambient (90 ± 6%) and low (93 ± 7%) DO. With TOTDMA, nitrogen recoveries were less under ambient (82 ± 5%) than low (97 ± 7%) DO. Oxygen recoveries under ambient DO were 88−97%, and the so-called unidentified product of dichloramine decomposition formed at about three-fold greater concentration under ambient compared to low DO, like NDMA, consistent with a DO limitation. Unidentified product formation stemmed from peroxynitrite decomposition products reacting with mono/dichloramine. For a 2:2:1 nitrogen/oxygen/chlorine atom ratio and its estimated molar absorptivity, unidentified product inclusion with uncertainty may close oxygen recoveries and increase nitrogen recoveries to 98% (ambient DO) and 100% (low DO).

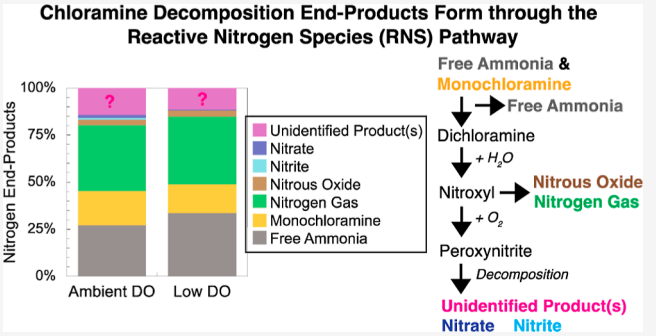

KEYWORDS: *chloramine chemistry, unidentified product, dissolved oxygen microelectrode interference, disinfection byproduct, N-nitrosodimethylamine, formation pathway*

INTRODUCTION

Chloramines are a commonly used secondary drinking water disinfectant in the United States because they form lower concentrations of regulated disinfection byproducts (DBPs),[1] and chloramine residuals are more persistent compared with free chlorine.[2] At pH levels typical in drinking water systems (pH 7−10),[3] monochloramine (NH_2Cl) is the predominant chloramine species and decomposes through dichloramine ($NHCl_2$) in the presence of total free ammonia ($TOTNH_3$ = $NH_4^+ + NH_3$) to nitrogen gas (N_2), nitrite (NO_2^-), and nitrate (NO_3^-).[4,5] Several reaction schemes and kinetic models have been proposed to capture the fate of free chlorine ($HOCl + OCl^-$) and chloramines under various drinking water conditions.[6−8] The unified (UF) model of chloramine chemistry[9] has been validated experimentally and captures chloramine speciation and stability under typical drinking water conditions. Table S1 shows the 14 reactions in the UF model (U1−U14), with U7−U9 revised based on our previous work demonstrating reactive nitrogen species (RNS) formed during $NHCl_2$ decomposition.[5] The unidentified intermediate, *I*, formed by $NHCl_2$ hydrolysis was shown to be nitroxyl (HNO) which reacts with dissolved oxygen (DO) to form peroxynitrite. U1−U10 are relevant to drinking water chloramination where excess $TOTNH_3$ is present. U11−U14 are relevant to breakpoint chlorination[10] and not considered in this study. U7−U10 are empirical redox reactions formulated to capture NH_2Cl and $NHCl_2$ concentrations over varied conditions[7,11] but do not account for minor nitrogenous species whose formation pathways may be important in DBP formation through reactive oxygen species and RNS.[4]

Received: September 29, 2023
Revised: December 18, 2023
Accepted: December 28, 2023
Published: January 18, 2024

Scheme 1. Proposed Reaction Scheme for the UF + RNS Model, Showing $NHCl_2$ Decomposition and NDMA Formation[a]

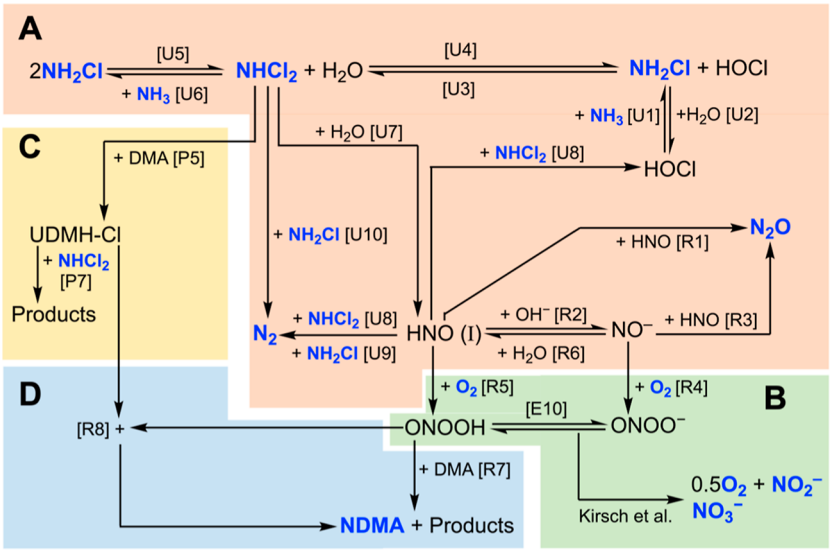

[a]Adapted from Pham et al.[5] and segmented into Pathways A–D based on DO and dimethylamine (DMA, DMA plus dimethylammonium cation, $DMAH^+$, pK_a = 10.73) presence. Pathway A (orange shading) represents DO-independent chloramine decomposition from $NHCl_2$ hydrolysis to HNO and ultimately N_2O and N_2. Pathway B (green shading) summarizes $ONOOH/ONOO^-$ formation and decomposition and is initiated by DO-dependent reactions, increasing Pathway B relevance under ambient vs low DO. Pathway C (yellow shading) is relevant upon DMA addition and is DO independent. Pathway D (blue shading) forms NDMA and requires DMA and DO-dependent $ONOOH/ONOO^-$ generation, making Pathway D more relevant under ambient vs low DO. Species in the blue font were measured in the current work.

In Scheme 1A, HNO dissociates to nitroxyl anion (NO^-), which is a kinetically controlled spin-forbidden reaction.[12] HNO/NO^- (hereinafter nitroxyl) can react with HNO to form nitrous oxide (N_2O),[13] a stable end-product in water,[14] that was missing from previous nitrogen mass balances on chloramine decomposition.[15] However, it is not yet known the extent to which N_2O closes the nitrogen mass balances. Nitroxyl can also react with (i) $NHCl_2$ to form N_2 and HOCl, (ii) NH_2Cl to form N_2, and (iii) DO which initiates Scheme 1B, forming the peroxynitrous acid/peroxynitrite anion ($ONOOH/ONOO^-$, hereinafter peroxynitrite) as an important intermediate. Peroxynitrite decomposes through RNS (e.g., $^{\bullet}NO_2$) and reactive oxygen species (e.g., $HO^{\bullet}$ and $CO_3^{\bullet-}$) to either nitrite (NO_2^-) plus half a mole of DO or NO_3^-, the distribution of which is pH-dependent.[16] Potential cross reactions between peroxynitrite and/or its decomposition products and species from the chloramine system are not in the UF + RNS model, and the extent to which these reactions may be important in DBP formation is unknown.

Peroxynitrite and/or its decomposition products were previously shown to react with total dimethylamine [TOTDMA = dimethylammonium cation, $DMAH^+$ plus dimethylamine (DMA), pK_a = 10.73], to form *N*-nitrosodimethylamine (NDMA, Scheme 1C,D).[17] NDMA is a nonhalogenated DBP associated with chloramination[18] and is classified by the United States Environmental Protection Agency as a probable human carcinogen.[19] TOTDMA is a common probe compound used to assess NDMA formation in chloramine systems.[5,17,18] With 10 μM-N TOTDMA and ambient DO, our previous work[5] showed uric acid, a peroxynitrite scavenger,[20] shutdown NDMA formation at pH 7, where NDMA final concentrations were the lowest. At pH 9, however, where NDMA formation was maximal, 160 μM uric acid decreased NDMA formation by only about half. Because greater uric acid concentrations increased chloramine decomposition, it was unfeasible to fairly demonstrate complete NDMA formation shutdown at pH 9 under ambient DO. We hypothesize that uric acid could not scavenge peroxynitrite and/or its decomposition products fast enough to shutdown NDMA formation under ambient DO. In this present work, therefore, we assessed uric acid scavenging under low DO conditions to slow peroxynitrite formation and assess NDMA formation through the RNS pathway. Nitroxyl and peroxynitrite are RNS and were previously integrated into the UF model[5] (Scheme 1) and referred to herein as the UF+RNS model. While this model accurately simulated $NHCl_2$, NH_2Cl, DO, and NDMA kinetics at pH 7–10, N_2O final concentrations were under-simulated at pH 7, 8, and 9 and oversimulated at pH 10.[5] Additionally, NDMA formation reactions in the UF+RNS model are empirical, leading to the possibility that other nitrogenous end-product(s) are missing in Scheme 1. Potential cross reactions with the chloramine system cannot be properly assessed until all of the stable end-products are accounted for experimentally.

One possible missing end-product that has yet to be considered in the UF+RNS model is the so-called unidentified product of dichloramine decomposition.[21] The unidentified product was first observed almost four decades ago as an ultraviolet (UV) absorbance-based interference while kinetically monitoring NH_2Cl and $NHCl_2$ at 231 and 295 nm.[7] Subsequent studies showed its accumulation paralleled total oxidant loss, absorbed maximally at about 245 nm, and was stable in water for weeks.[21−23] Photolysis destroyed the unidentified product and yielded two moles of chloride per one mole of NO_3^- along with some NO_2^-, demonstrating that it contained nitrogen (N) and chlorine (Cl). While the structure of the unidentified product remains unknown, its concentration can be estimated using its estimated molar absorptivity (ε) of 5000 $M^{-1}\cdot cm^{-1}$ at 245 nm and assuming one Cl atom per molecule.[21] Like NDMA,[5] we hypothesize that the

https://doi.org/10.1021/acs.est.3c08088
Environ. Sci. Technol. 2024, 58, 2048−2057

unidentified product forms through the RNS pathway during $NHCl_2$ decomposition. Previously reported $NHCl_2$ decomposition studies have been completed under ambient DO.[6,7,11,24] Potential cross reactions may exist between reactive oxygen species and RNS and/or their decomposition products and species such as NH_2Cl, $NHCl_2$, and $TOTNH_3$.[25−27] Assessing $NHCl_2$ decomposition under low DO would slow peroxynitrite formation and simplify Scheme 1 primarily to Scheme 1A (no TOTDMA) or Scheme 1A,C (with TOTDMA). N and oxygen (O) mass balances under ambient and low DO could therefore provide information about the relative importance of the unidentified product compared to other $NHCl_2$ decomposition end-products and insights into its formation pathway to spur future work aimed at revealing its structure and assessing its potential public health risk.

The current work assesses the UF+RNS model completeness in terms of N- and O-containing end-products and assesses the role of chloramine disinfectant chemistry in nitrogenous DBP formation. If the UF+RNS model is incomplete, then it will not be robust regarding the development of generalizable DBP control strategies for chloramine systems. Here, we seek to identify all the stable end-products of $NHCl_2$ decomposition and identify potential missing end-products and reactions to be interrogated in future work. Scheme 1 was divided into (1) Pathways A and C, which are DO independent, and (2) Pathways B and D, which require DO to initiate. Under ambient DO (~500 μM-O) and no added TOTDMA, Pathways A and B are relevant, with Pathway B limited under low DO (≤40 μM-O). With TOTDMA, Pathways A−D are relevant under ambient DO with Pathways B and D limited under low DO. To assess peroxynitrite as the critical NDMA formation intermediate at pH 9 where NDMA final concentrations are maximal,[5] low DO experiments were completed with uric acid, a peroxynitrite scavenger.[28−30] N and O mass balances were then completed at pH 9, following $NHCl_2$ decomposition at initial concentrations of 200, 400, and 800 μeq $Cl_2 \cdot L^{-1}$ under ambient and low DO in the absence and presence of 10 μM-N TOTDMA addition (ambient DO ± DMA and low DO ± DMA). N_2, $TOTNH_3$, and NH_2Cl were expected to be the primary N-containing end-products and were measured along with N_2O, NO_2^-, and NO_3^-. For two treatments with the addition of TOTDMA, NDMA was also measured. Last, to assess its potential importance in closing N- and O-mass balances, unidentified product concentrations were estimated at the greatest $NHCl_2$ dose (800 μeq $Cl_2 \cdot L^{-1}$) to maximize unidentified product formation under ambient and low DO without DMA present to prevent DMA interfering with UV absorbance measurements.

MATERIALS AND METHODS

Experiments were performed at room temperature (~23 °C). The reagents used are detailed in the Supporting Information, S2.1. This section's remainder details peroxynitrite quenching with uric acid, ambient DO experiments, low DO experiments, and N and O mass balances.

Peroxynitrite Quenching with Uric Acid and NDMA. A peroxynitrite quenching experiment was completed using uric acid under low DO (≤40 μM-O, see Low DO Experiments) at pH 9 in 40 mM borate buffer [pK_a = 9.14,[31] referred to herein as total borate, $TOTBO_3 = H_3BO_3 + B(OH)_4^-$, see Supporting Information, S2.2] with initial concentrations of 800 μeq $Cl_2 \cdot L^{-1}$ $NHCl_2$ (see Supporting Information, S2.3) and 10 μM-N TOTDMA. NDMA final concentrations at 24 h were measured in solutions dosed with uric acid at 20, 40, 80, 120, and 160 μM. These uric acid concentrations were shown to not impact NH_2Cl and $NHCl_2$ profiles in our prior work.[5] NDMA was identified and quantified using electrospray ionization gas chromatography−mass spectrometry with an LoQ of 0.100 μM-N, as detailed previously.[5]

Ambient DO Experiments. As shown in Scheme S1, ambient DO experiments ± DMA were prepared in triplicate in two 40 mL headspace-free amber glass vials (A,C) and one 20 mL nominal crimp seal vial (B) with 12.5 mL of solution and 7.5 mL of headspace. All vials contained water buffered at pH 9 with 40 mM $TOTBO_3$ and dosed with $NHCl_2$ at 200, 400, or 800 μeq $Cl_2 \cdot L^{-1}$. After 24 h (e.g., following complete $NHCl_2$ decomposition at pH 9),[5] vial A was analyzed for NO_2^- and NO_3^- (Supporting Information, S2.4) and for the subset of vials containing 10 μM-N TOTDMA, NDMA; vial B was used for N_2 quantification (Supporting Information, S2.5), with the triplicate consisting of initial ^{15}N ratios for $NHCl_2$ of 0.10, 0.15, and 0.20 for each dosed $NHCl_2$ concentration; and vial C was analyzed for pH and $TOTNH_3$ (Supporting Information, S2.6 for $TOTNH_3$ quantification and $NHCl_2$ interference), NH_2Cl and total chlorine (Supporting Information, S2.3), N_2O and DO microelectrode measurements (Supporting Information, S2.7 for quantification and chloramine interference on DO microelectrode), and, for the subset of vials without added 10 μM-N TOTDMA, UV absorbance spectra (200−600 nm) to estimate the unidentified product concentration (see Supporting Information, S2.8).

Low DO Experiments. $NHCl_2$ decomposition and nitrogen end-product formation were studied under low DO ± DMA in a glovebox (Labconco, model 50700-00) with an ultrahigh-purity nitrogen atmosphere. The workflow was like the ambient DO experiments (Scheme S1), and the purging procedure to minimize DO in solutions is detailed in Supporting Information, S2.9. Prior to each experiment, all stock solutions and Milli-Q water were checked to ensure that initial DO microelectrode (Unisense) readings were ≤40 μM-O. NH_2Cl and $NHCl_2$ stock solutions were prepared inside the glovebox following the same procedure as for ambient DO experiments. Approximately 10 mL of NH_2Cl and $NHCl_2$ stock solutions was transferred into a 25 mL amber glass vial and taken outside for quantification with the UV−vis spectrophotometer (Supporting Information, S2.3). The NH_2Cl solution was only used for $NHCl_2$ preparation, and the resultant $NHCl_2$ solution was only used when measured concentrations were within ±5% of target concentrations. Low DO samples were prepared following Scheme S1 for ambient DO experiments. After 24 h, N_2O concentrations were measured for 7−10 min per sample inside the glovebox using a N_2O microelectrode (Unisense). All remaining sample vials were removed from the glovebox for measurement of pH, $TOTNH_3$, NH_2Cl, N_2, NO_2^-, and NO_3^-, as detailed previously. Chloramine species measured using wet chemistry methods were completed within 10 min after the vial was opened to minimize possible DO interferences. For the subset of vials with 10 μM-N TOTDMA added, the NDMA final concentrations were also measured.

N and O Mass Balances. Twelve N mass balances were calculated in triplicate, comprising three initial $NHCl_2$ concentrations (200, 400, and 800 μeq $Cl_2 \cdot L^{-1}$) and four experimental treatments (ambient DO ± DMA and low DO ±

https://doi.org/10.1021/acs.est.3c08088
Environ. Sci. Technol. 2024, 58, 2048−2057

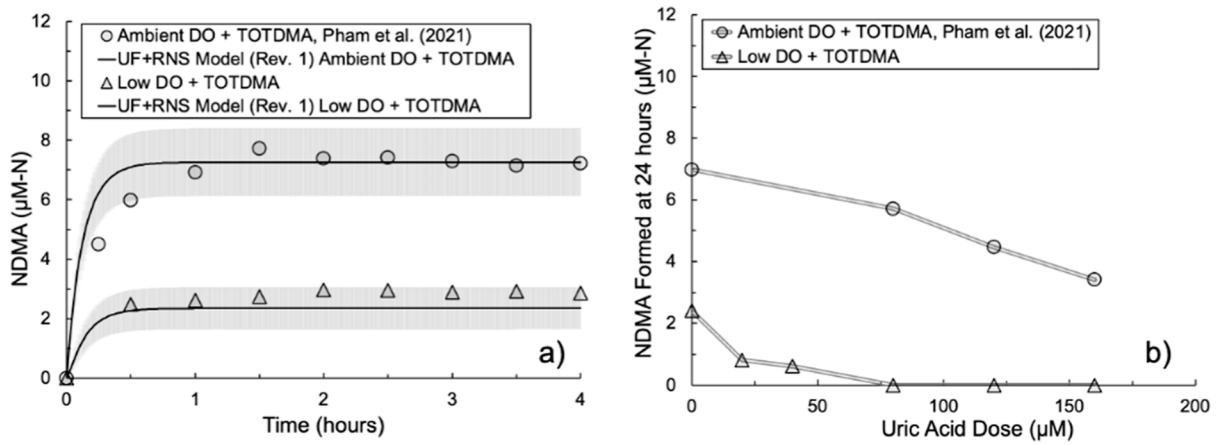

Figure 1. NDMA formation at pH 9 in 40 mM $TOTBO_3$ with 10 μM-N TOTDMA and 800 μeq $Cl_2 \cdot L^{-1}$ $NHCl_2$ under ambient DO (~500 μM-O, reported previously[5]) and low DO (≤40 μM-O, this work). (a) Kinetic NDMA concentrations in which points are measured values, lines are UF +RNS model (rev. 1) simulations, and gray-shaded regions encompass one standard error in the estimated model rate constants and (b) NDMA final concentrations at 24 h as a function of uric acid dose under the ambient and low DO; lines illustrate trends.

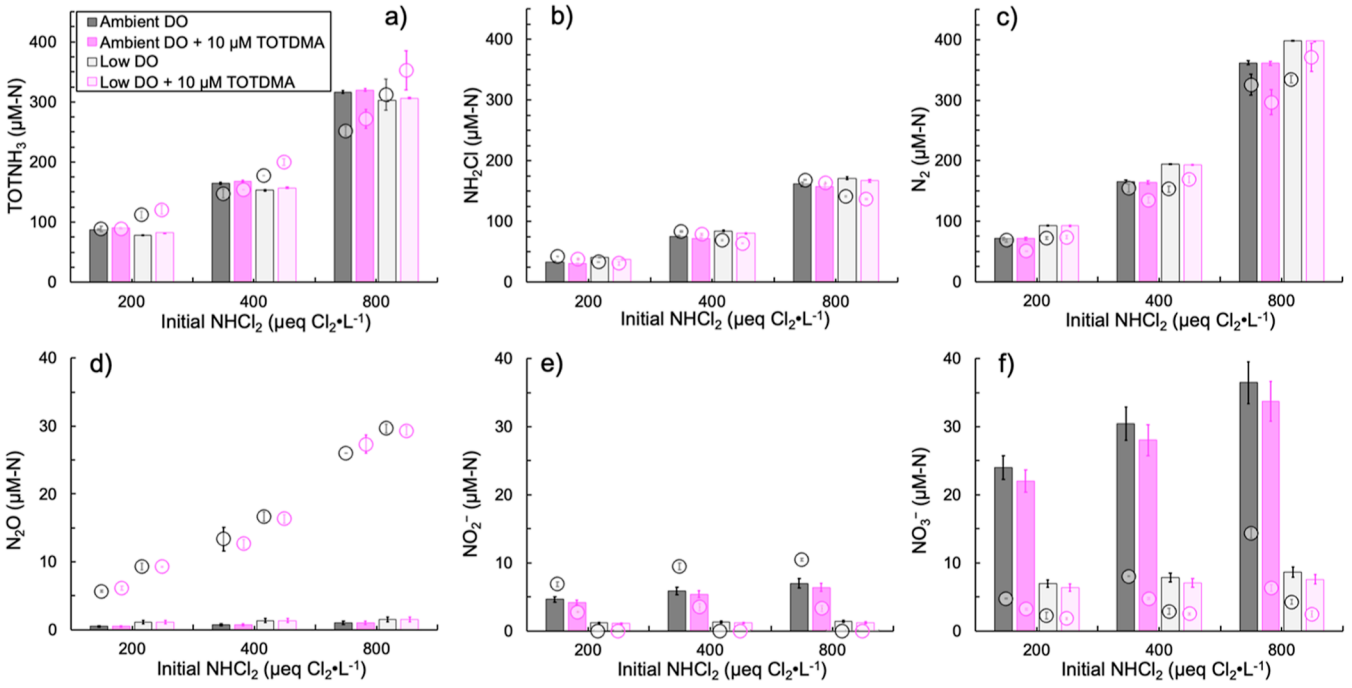

Figure 2. Measured (circles) and UF+RNS model (rev. 1) simulated (bars) final concentrations of the major nitrogen containing end-products (a) $TOTNH_3$, (b) NH_2Cl, and (c) N_2 and minor nitrogen containing end-products (d) N_2O, (e) NO_2^-, and (f) NO_3^- after a 24 h reaction time in waters dosed with ca. 200, 400, and 800 μeq $Cl_2 \cdot L^{-1}$ $NHCl_2$ buffered at pH 9 with 40 mM $TOTBO_3$ under ambient DO (~500 μM-O, dark-shaded bars) and low DO (≤40 μM-O, light-shaded bars) without TOTDMA addition (dark gray and light gray) and with 10 μM-N TOTDMA addition (dark magenta and light magenta). Error bars on the measured values represent the 95% confidence interval on either side of the mean measured concentrations (n = 3); error bars on model-simulated values represent one standard error in the model parameter estimates.

DMA). Six O mass balances were calculated, composed of the same initial $NHCl_2$ concentrations but for ambient DO experiments only as the initial DO for low DO experiments were ≤40 μM-O. The initial total nitrogen concentration for each condition was determined by summing measured initial $NHCl_2$ and calculated $TOTNH_3$ concentrations. A calculated $TOTNH_3$ concentration was used because the initial $TOTNH_3$ could not be accurately measured with the presence of $NHCl_2$ (Supporting Information, S2.6). Final total nitrogen concentrations were measured after 24 h, corresponding to complete $NHCl_2$ decomposition,[5] and consisted of summing measured μM-N concentrations of $TOTNH_3$, NH_2Cl, N_2, N_2O, NO_2^-, NO_3^-, and, when 10 μM-N TOTDMA was added, NDMA. For one 800 μeq $Cl_2 \cdot L^{-1}$ $NHCl_2$ experiment under ambient and low DO without TOTDMA, the unidentified product concentration was estimated using absorbance at 245 nm in units of μM-Cl after accounting for NH_2Cl, NO_2^-, NO_3^-, and NH_3, as detailed in Supporting Information, S2.8. N_2O, $ONOO^-$, and carbonate species had negligible absorbance at 245 nm (Supporting Information, S2.8 and Figure S1) and were thus ignored in the unidentified product quantitation.

https://doi.org/10.1021/acs.est.3c08088
Environ. Sci. Technol. 2024, 58, 2048−2057

RESULTS AND DISCUSSION

Impact of Buffer on Nitrogenous End-Product Speciation. S3.1 in the Supporting Information and Tables S2 and S3 demonstrate that 20−40 mM borate buffer concentration did not impact final concentrations of N-containing end-products in Scheme 1. To match the pH 9 buffer used in our previous work,[5] 40 mM $TOTBO_3$ was used for all experiments in this study.

DO Microelectrode Concentrations Corrected for NH_2Cl and $NHCl_2$ Interferences. S3.2 in the Supporting Information and Figure S2 show $NHCl_2$ and NH_2Cl concentrations produced positive interferences on the DO microelectrode signal that were directly proportional to $NHCl_2$ and NH_2Cl concentrations. S3.3 and Figure S3 show initial DO decreased by about 75 μM-O at each pH level to 484−518 μM-O (Figure S3, corrected DO) compared to measured DO concentrations from our previous work (Figure S3, measured DO).[5] These corrections about doubled the rate constants for three reactions downstream of DO (S3.4 and Table S4) but did not impair the NH_2Cl, $NHCl_2$, and NDMA concentration simulations made using Aquasim[32] (Table S5) or the interpretations made regarding the UF+RNS model.[5] This revised UF+RNS model was used to simulate the species in the N and O mass balances and is referred to herein as the UF +RNS model (rev. 1).

Peroxynitrite Scavenging Shutdown NDMA Formation at pH 9 under Low DO. Figure 1a shows NDMA concentrations at pH 9 for ambient DO from our previous study[5] and that from low DO collected in this work.

The measured NDMA concentrations tracked closely with the UF+RNS model (rev. 1) simulations. Following Scheme 1, peroxynitrite formation is directly dependent on the DO concentration; therefore, lower DO was consistent with decreased NDMA. For ambient DO (initial DO ∼ 500 μM-O), NDMA reached a near-constant level of about 7 μM-N after about 1 h. Compared to low DO (initial DO ∼ 40 μM-O), NDMA concentrations plateaued at about 2 μM-N after about 0.5 h. Decreased NDMA final concentrations under low DO were similar to that reported by Schreiber and Mitch[17] and Yang et al.[33] and are consistent with a DO limitation.

Figure 1b shows NDMA final concentrations at pH 9 for ambient and low DO as a function of uric acid dose up to 160 μM, which was the greatest uric acid dose shown previously not to impact chloramine decomposition.[5] For ambient DO, NDMA final concentrations decreased from about 7 to 4 μM-N whereas, under low DO, NDMA final concentrations decreased from about 2 μM-N to below the limit of quantification of 0.100 μM-N at uric acid doses of about 80 μM and greater. This supports peroxynitrite as a critical intermediate in the NDMA formation pathway in chloramine systems and indicates that uric acid scavenging could be outcompeted by NDMA formation reactions under ambient DO, as observed in our previous work.[5] This result further supports all NDMA formation occurring through the RNS pathway, as shown in Scheme 1.

Nitrogenous End-Products of $NHCl_2$ Decomposition. Figure 2 shows final concentrations of six nitrogenous end-products as a function of initial $NHCl_2$ concentrations at pH 9 under ambient and low DO ± DMA and their companion UF +RNS model (rev. 1) simulated final concentrations. S3.5 and Figure S4 show measured and simulated NDMA final concentrations with added TOTDMA only. Tables S6 and S7 show concentration data used to produce Figures 2 and S4.

Measured $TOTNH_3$, NH_2Cl, and N_2 final concentrations increased with initial $NHCl_2$ concentration and were the major N-containing end-products in accordance with the UF model.[9,11,34] At the 800 μeq $Cl_2 \cdot L^{-1}$ $NHCl_2$ dose, measured $TOTNH_3$ and N_2 final concentrations were between 252 and 371 μM-N, and NH_2Cl final concentrations were about half at 137−168 μM-N (Figure 2). Measured N_2O, NO_2^-, and NO_3^- final concentrations also increased with the initial $NHCl_2$ concentration but were comparatively minor with maximum final concentrations of 30, 10, and 14 μM-N, respectively. Similarly, Figure S4 shows that measured NDMA final concentrations increased with initial $NHCl_2$ concentration with a maximum NDMA formation of about 7 μM-N.

Figure 2a shows that measured $TOTNH_3$ final concentrations were greater under low DO compared to ambient DO. At the 800 μeq $Cl_2 \cdot L^{-1}$ $NHCl_2$ dose, measured $TOTNH_3$ was greater under low DO by about 20% or 60 μM-N (no TOTDMA) and 25% or 80 μM-N (with TOTDMA). Similar trends existed for all three $NHCl_2$ doses, suggesting that $TOTNH_3$ reacted with peroxynitrite or its decomposition products. $HO^\bullet$ and $NO_2^\bullet$ have been demonstrated to form during peroxynitrite decomposition,[35−37] and a reaction between NH_3 and $HO^\bullet$ was reported in the advanced oxidation literature[25−27] to yield $NH_2^\bullet$ which can directly react with (i) NH_2Cl to form $NHCl^\bullet$ and NH_3, (ii) $NHCl_2$ to form $NCl_2^\bullet$ and NH_3, (iii) $HO^\bullet$ to form NH_2OH, (iv) DO to form $NH_2O_2^\bullet$, and (v) $NH_2^\bullet$ to form N_2H_4. Many of these species are intermediates and, in turn, may react with various species present in chloramine systems. CO_2 proper can alter peroxynitrite decomposition and form species which could be relevant in DBP formation. At near neutral pH, dissolved inorganic carbon (DIC) accelerated $ONOO^-$ decomposition in a concentration-dependent manner, and pH-jump experiments indicated a direct reaction with CO_2 proper and not carbonate species.[38] However, DIC was 2 mM in the low and ambient DO experiments (see Supporting Information, S2.3), rendering any adventitious DIC negligible (e.g., dissolution of CO_2 from the ambient atmosphere or CO_2 evolution from the samples in the glovebox). The $ONOO^-$ reaction with CO_2 proper is fast and forms a short-lived intermediate ($ONOOCO_2^-$) that undergoes homolytic cleavage of the peroxide bond to produce carbonate radical ($CO_3^{\bullet-}$) and nitrogen dioxide ($NO_2^\bullet$) in ca. 30% yield[39] and heterolytic cleavage to yield NO_2^+.[38] $CO_3^{\bullet-}$, $NO_2^\bullet$, and NO_2^+ can oxidize, nitrate, and hydroxylate other species and therefore are candidates for future investigations of cross reactions with the chloramine system. While the UF+RNS model (rev. 1), simulated $TOTNH_3$ concentrations were ±20% of their measured values, the model generally oversimulated ambient DO and undersimulated low DO conditions.

Figure 2b shows that measured NH_2Cl final concentrations were less for low DO compared to ambient DO ± DMA by about 20% or 30 μM-N for the 800 μeq $Cl_2 \cdot L^{-1}$ $NHCl_2$ dose. Under low DO, less NH_2Cl (Figure 2b) was consistent with more $TOTNH_3$ (Figure 2a), suggesting that less HOCl was released under low DO or HOCl was consumed in another reaction. However, the 60−80 μM-N additional $TOTNH_3$ measured under low DO was over double the measured decrease in NH_2Cl (30 μM-N). The UF+RNS model (rev. 1) accurately simulated NH_2Cl concentrations for ambient DO but oversimulated NH_2Cl for low DO by as much as 20%.

https://doi.org/10.1021/acs.est.3c08088
Environ. Sci. Technol. 2024, 58, 2048−2057

Therefore, low DO may have slowed the $TOTNH_3$ consuming reactions and/or cross reactions that occurred between RNS and $NHCl_2$ and/or NH_2Cl.

Figure 2c shows that measured N_2 final concentrations were similar between ambient and low DO without TOTDMA for all three $NHCl_2$ doses; this was unexpected as Scheme 1B was restricted under low DO. With added TOTDMA, however, measured N_2 final concentrations for ambient DO were less than low DO by 23, 34, and 75 μM-N or 20−32% for $NHCl_2$ doses of 200, 400, and 800 μeq $Cl_2 \cdot L^{-1}$. This result follows Scheme 1, in which more N_2 forms when Scheme 1B is restricted. The UF + RNS model (rev. 1) generally oversimulated measured N_2 formation by up to 30%, with greater N_2 simulated for low DO. This result is consistent with excess HNO reacting with NH_2Cl or $NHCl_2$ to form N_2 by U8 or U9 instead of reacting with DO to form peroxynitrite and/or HNO to additional N_2O. However, this trend was only observed for measured N_2 concentrations with 10 μM-N TOTDMA.

Figure 2d shows that final measured N_2O concentrations increased from about 5−9 μM-N at the 200 μeq $Cl_2 \cdot L^{-1}$ $NHCl_2$ dose to 25−30 μM-N at the 800 μeq $Cl_2 \cdot L^{-1}$ $NHCl_2$ dose. Measured N_2O formation was greater for low DO compared to ambient DO by about 2−4 μM-N (7−12% increase at the 800 μeq $Cl_2 \cdot L^{-1}$ $NHCl_2$ dose). This result is consistent with Scheme 1, in which the amount of HNO siphoned away from N_2O formation is directly proportional to the product of the DO concentration and the second-order rate constants for R4 and R5. Notably, the model-simulated N_2O final concentrations were less than 2 μM-N and insensitive to initial $NHCl_2$ and DO concentrations, indicating a potential deficiency in the UF+RNS model (rev. 1). One candidate for revision is the R5 second-order rate constant in Scheme 1B. While the R4 rate constant has been measured as 2.7×10^9 $M^{-1} \cdot s^{-1}$,[12] reports for R5 range from $0.3-1.8 \times 10^4$ $M^{-1} \cdot s^{-1}$,[40] with the upper end value used in our prior work[5] and the UF+RNS model (rev. 1). A second candidate is the addition of the cross reaction between NH_3 and $HO^{\bullet}$ to form NH_2OH which can react with either HOCl or NH_2Cl to form HNO[14] that reacts with itself and its conjugate base (NO^-) to form N_2O.[13] However, N- and O mass balances are first needed to assess if there are missing stable end-products in Scheme 1.

Figure 2e shows that measured NO_2^- final concentrations increased from about 7 to 10 μM-N for ambient DO as initial $NHCl_2$ concentrations increased from 200 to 800 μeq $Cl_2 \cdot L^{-1}$. With added TOTDMA, NO_2^- final concentrations were about 3 μM-N for ambient DO. The difference of about 4−7 μM-N in NO_2^- final concentrations under ambient DO upon 10 μM-N TOTDMA addition was approximately equal to the measured final NDMA (Figure S4). It is possible that NDMA formation interrupted the NO_2^- formation pathway during peroxynitrite decomposition as opposed to a direct reaction with peroxynitrite proper, as currently implemented empirically in the UF+RNS model (rev. 1). Under low DO, NO_2^- was below the level of detection, which supports the assertion that NO_2^- did not form in Scheme 1A but rather in Scheme 1B as a product of peroxynitrite decomposition. NO_2^- was adequately simulated by the UF+RNS model (rev. 1) for the four experimental conditions and three $NHCl_2$ doses.

Figure 2f shows that final measured NO_3^- concentrations increased from about 5 to 14 μM-N for ambient DO as initial $NHCl_2$ concentrations increased from 200 to 800 μeq $Cl_2 \cdot L^{-1}$. With added TOTDMA, NO_3^- final concentrations were about 3 to 5 μM-N for ambient DO, indicating that 10 μM-N TOTDMA addition interrupted the NO_3^- formation pathway during peroxynitrite decomposition. Coupled with the findings in Figure 2e, NDMA formation may have stemmed from peroxynitrite proper or its decomposition products common to the NO_2^- and/or NO_3^- formation pathways. Under low DO, the NO_3^- final concentrations were 2 to 4 μM-N. NO_3^- was oversimulated under all conditions, by about 19 to 30 μM-N under ambient DO and about 4 μM-N under low DO. It is likely that species from the chloramine system (e.g., $NHCl_2$, NH_2Cl, and HOCl) interrupted the NO_3^- formation pathway within the peroxynitrite decomposition reaction scheme.[16] CO_2 can alter the amounts of NO_2^- and NO_3^- formed. Sharpless and Linden[41] found that 1 mM DIC decreased NO_2^- yields from $ONOO^-$ decomposition during UV photolysis of NO_3^- at pH 8. Figure S5 shows UF+RNS model (rev. 1) simulations of NO_2^- and NO_3^- yields vs DIC for ambient and low DO. NO_3^- increased while NO_2^- decreased with increasing DIC, the slopes of which were larger at 0−3 mM DIC compared to 3−30 mM DIC. The total NO_2^- plus NO_3^- was near constant with DIC, and at 2 mM (e.g., the DIC of the ambient and low DO samples), NO_3^- was about 85% of the total while NO_2^- was 15%. DIC alters the peroxynitrite decomposition pathway, which could impact DBP formation as the species involved in NO_3^- formation differ from those of NO_2^-.[16]

Figure S4 shows measured NDMA final concentrations increased from about 5 to 7 μM-N for ambient DO as initial $NHCl_2$ concentrations increased from 200 to 800 μeq $Cl_2 \cdot L^{-1}$. For low DO, measured NDMA final concentrations were about 2 μM-N at all three initial $NHCl_2$ concentrations, consistent with a DO limitation. While the UF+RNS model (rev. 1) simulations were accurate, future work is needed to revise the empirical rate expressions (Table S4) into mechanistic implementations following identification of the nitrosating agent(s).

DO Consumed during $NHCl_2$ Decomposition. Table S8 shows initial measured DO, final measured DO, and calculated DO consumed based on the initial minus final DO plus one-half the final NO_2^- per Scheme 1B for ambient DO and ambient DO + DMA. For 200, 400, and 800 μeq $Cl_2 \cdot L^{-1}$ initial $NHCl_2$, the DO consumed was 42, 66, and 101 μM-O for ambient DO and 26, 42, and 59 μM-O for ambient DO + DMA, respectively. Following Scheme 1B,D, the addition of 10 μM-N TOTDMA interrupted NO_2^- formation, with differences in NO_2^- of 8.2, 11.9, and 14.4 μM-O for the 200, 400, and 800 μeq $Cl_2 \cdot L^{-1}$ initial $NHCl_2$ doses (Table S6, with NO_2^- concentrations in μM-N multiplied by two to convert to μM-O). The reaction between $NHCl_2$ and DMA (Scheme 1C) does not consume DO, which may explain the additional DO consumption without TOTDMA where greater amounts of HNO form and react with DO (Scheme 1B). N and O mass balances were assessed next to determine the completeness of the end-products shown in Scheme 1.

N and O Mass Balances for $NHCl_2$ Decomposition at pH 9. Figure 3 shows the N and O mass balances for three initial $NHCl_2$ concentrations and four experimental treatments.

Table S9 shows the nitrogen recovery ratio (NRR) for the three replicates and four treatments at initial $NHCl_2$ concentrations of 200, 400, and 800 μeq $Cl_2 \cdot L^{-1}$, and Table S10 shows the corresponding two-way analysis of variance (ANOVA) that was used to compare the NRR among the

https://doi.org/10.1021/acs.est.3c08088
Environ. Sci. Technol. 2024, 58, 2048−2057

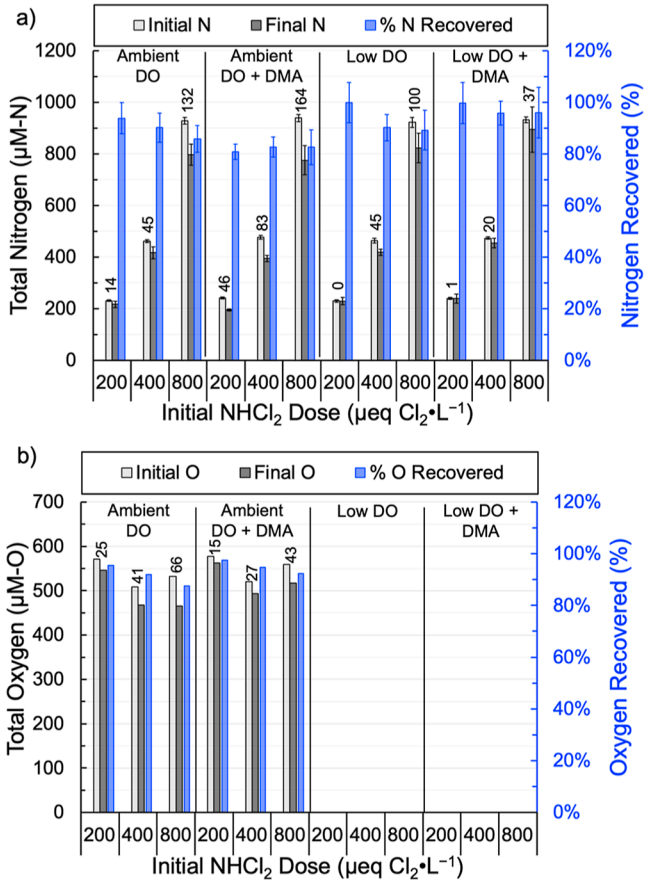

Figure 3. $NHCl_2$ complete decomposition mass balances on (a) nitrogen (N) and (b) oxygen (O) for waters buffered at pH 9 with 40 mM $TOTBO_3$ ± 10 μM-N TOTDMA addition and dosed with 200, 400, or 800 μeq $Cl_2 \cdot L^{-1}$ $NHCl_2$ under ambient DO (~500 μM-O) and low DO (≤40 μM-O). N mass balances in panel (a) show the initial total N (Initial N) from the sum of initial measured $NHCl_2$ and calculated $TOTNH_3$; final total N (Final N) from the sum of final measured $TOTNH_3$, NH_2Cl, N_2, N_2O, NO_2^-, NO_3^-, and NDMA; and the percent N recovered (% N recovered) from dividing the final by initial total N (see Tables S6 and S7). Error bars in panel (a) represent 95% confidence intervals calculated using error propagation from triplicate experiments. O mass balances in panel (b) show the initial total O (initial O) from the initial measured chloramine species-corrected DO microelectrode measurement; final total O (final O) from the sum of the final measured chloramine species-corrected DO microelectrode measurement plus the O required from DO (i.e., not from water) based on Scheme 1 for the final measured NO_2^- (1 μM-O/1 μM-N), NO_3^- (2 μM-O/1 μM-N), and NDMA (0.5 μM-O/1 μM-N); and the percent O recovered (% O recovered) from dividing the final by initial total O (see Table S8). Error bars are not shown in panel (b) because DO concentrations were measured once (n = 1). No oxygen data were shown for low DO because the initial DO was less than 40 μM-O which could not be reliably quantified because of the chloramine species interferences (see Figure S2). Numbers above bars represent the average N and O concentrations unaccounted for in the final totals, with errors not shown numerically for clarity.

different treatments. Significant differences (p < 0.0001) were observed among treatment groups with the aggregated NRR as follows for treatment (NRR ± 95% CIs): ambient DO + DMA (0.84 ± 0.05) < ambient DO (0.90 ± 0.06) ≅ low DO (0.93 ± 0.07) < low DO + DMA (1.00 ± 0.08). While complete N recovery was achieved within error for low DO, N-containing species other than $TOTNH_3$, NH_2Cl, N_2, N_2O, NO_2^-, NO_3^-, and NDMA (Scheme 1) comprise the remainder of the N mass balances for ambient DO. At the 800 μeq $Cl_2 \cdot L^{-1}$ initial $NHCl_2$ concentration, Figure 3a shows missing N totaled 132 ± 51 and 164 ± 66 μM-N in ambient DO and ambient DO + DMA, respectively, compared to 100 ± 74 and 37 ± 92 μM-N in low DO and low DO + DMA, respectively. Figure 3b shows that oxygen recovery ranged from 88−97% for ambient DO and ambient DO + DMA. At the 800 μeq $Cl_2 \cdot L^{-1}$ initial $NHCl_2$ concentration, the missing μM-O totaled 66 and 43 μM-O in ambient DO and ambient DO + DMA, respectively. Therefore, under ambient DO, missing N was about 1.2−5.4 times greater than missing O after accounting for measurement errors. The amount of N and O that could be accounted for in the unidentified product is assessed next.

Unidentified Product Estimates and Importance in N and O Mass Balances. Table 1 shows estimated unidentified product formation from 800 μeq of $Cl_2 \cdot L^{-1}$ $NHCl_2$ decomposition at pH 9 in 40 mM $TOTBO_3$ under ambient and low DO calculated using the absorbance method previously described.

Based on the absorbance at 245 nm (A_{245}) and measured NH_3, NH_2Cl, NO_2^-, and NO_3^- concentrations, unidentified product formation was estimated (assuming 1 Cl atom in the unidentified product) to be 30.6 and 9.9 μM-Cl under ambient and low DO, respectively. Despite the relatively large ε of $ONOO^-$ at 245 nm (1150−1750 $M^{-1} \cdot cm^{-1}$),[44] peroxynitrite species (pK_a = 6.8)[45] did not interfere with unidentified product quantification because the UF+RNS model (rev. 1) indicated that they were fully decomposed after about 1 h (see Figure S1), whereas the absorbance spectra were collected after 24 h. Assuming 1 or 2 mol of N, O, and Cl in the unidentified product, as speculated by others,[21] its formation ranges were 15.3−61.2 and 5.0−19.8 μM-N or −O under ambient and low DO, respectively. These final unidentified product concentrations were like the other minor N-containing species concentrations in Figure 2 (e.g., N_2O, NO_2^-, and NO_3^-) and Figure S4 (e.g., NDMA), illustrating the need to determine the structure of the unidentified product and quantify it kinetically prior to further revision of the UF+RNS model (rev. 1).

The DO consumption could not be accurately measured under low DO due to the magnitude of $NHCl_2$ interference on the DO microelectrode (Figure S2) relative to the initial DO (≤40 μM-O). However, for the 800 μeq $Cl_2 \cdot L^{-1}$ $NHCl_2$ dose, the unidentified product estimate (5.0−19.8 μM-O) and measured final NO_2^- (not detected, Table S6) and NO_3^- (4.3 μM-N, Table S6 multiplied by two to convert to 8.6 μM-O per Scheme 1) concentrations indicate that the initial DO must have been at least 13.6−28.4 μM-O. In comparison, DO consumed for the corresponding ambient DO was 101 μM-O (Table S8), which is about 3.6−7.4 times greater. This range is in line with the approximate three-fold difference in the unidentified product concentration between ambient and low DO (Table 1) and consistent with a DO limitation under low DO.

IMPLICATIONS

As all NDMA formation at pH 9 occurred through the RNS pathway (Figure 1b), N and O mass balances during $NHCl_2$ decomposition were completed to assess the contribution of this pathway to N and O-containing end-products. $TOTNH_3$, NH_2Cl, and N_2 were major N-containing end-products while

https://doi.org/10.1021/acs.est.3c08088
Environ. Sci. Technol. 2024, 58, 2048−2057

Table 1. Estimated Unidentified Product Formation from Complete Decomposition of 800 μeq $Cl_2 \cdot L^{-1}$ $NHCl_2$ in 40 mM $TOTBO_3$[a]

parameter	ε_{245}	treatment		
	$M^{-1} \cdot cm^{-1}$	units	ambient DO	low DO
total measured absorbance at 245 nm ($A_{245,Total}$)	NA	AU	0.228	0.112
NH_3	0.12[42]	μM-N (AU)	252 (3.0×10^{-5})	312 (3.7×10^{-5})
NH_2Cl by indophenol	445[43]	μM-Cl_2 (AU)	165 (0.073)	140 (0.062)
NO_2^-	91.9[42]	μM-N (AU)	10.5 (9.6×10^{-4})	<0.71 (<6.5×10^{-5})
NO_3^-	33.3[42]	μM-N (AU)	14.3 (4.8×10^{-4})	4.3 (1.4×10^{-4})
measured absorbance at 245 nm from known chemicals ($A_{245,Sum}$)	NA	AU	0.0749	0.0625
measured absorbance at 245 nm attributed to the unidentified product ($A_{245,UP}$)	NA	AU	0.153	0.0495
unidentified product (1 mol Cl)	5000[21]	μM-Cl	30.6	9.9
unidentified product (2 mol N or O and 1 mol Cl)	NA	μM-N or O	61.2	19.8
unidentified product (1 mol N or O and 2 mol Cl)	NA	μM-N or O	15.3	5.0
missing N ± 95% CI, Figure 3a	NA	μM-N	132 ± 51	100 ± 74
missing O, Figure 3b	NA	μM-O	66	ND

[a]At pH 9 under ambient DO (~500 μM-O, DO) and low DO (≤40 μM-O) calculated with molar absorptivity values at 245 nm (ε_{245}). AU—absorbance units; NA—not applicable; and ND—not determined because the initial DO was ≤40 μM-O and could not be reliably measured due to the chloramine species interferences (see Figure S1).

N_2O, NO_2^-, NO_3^-, and (in the presence of TOTDMA) NDMA, were minor N-containing end-products (Figures 2 and S4). The resulting mass balances showed closures between 82 ± 5% (ambient DO + DMA) and 97 ± 7% (low DO + DMA) for N (Table S9) and 88−97% for O (Figure 3b). The shutdown of NDMA formation under low DO by scavenging peroxynitrite (Figure 1b) supports the assertion that all NDMA formation occurred through the RNS pathway. N and O mass balances completed during $NHCl_2$ decomposition under ambient and low DO showed that the unidentified product was DO limited and formed from the RNS pathway. The unidentified product is not in the UF+RNS model (rev. 1), but its structure first needs to be revealed to facilitate the kinetic measurements necessary to incorporate it into the model. For ambient and low DO at 800 μeq $Cl_2 \cdot L^{-1}$, assuming an atom ratio of 2:2:1 for N/O/Cl, including the unidentified product in the N mass balances increases closure to 93 ± 5% (ambient DO) and 92 ± 8% (low DO). Therefore, unidentified product inclusion with uncertainty may close oxygen mass balances and increase nitrogen recoveries to 98% (ambient DO) and 100% (low DO). Unidentified product formation decreased about three-fold under low DO (Table 1), like NDMA (Figure S4), consistent with a DO limitation, implicating peroxynitrite and/or its decomposition products. Given the UF+RNS model (rev. 1) oversimulated NO_3^- by about 20 and 5 μM-N (Figure 2f) under ambient and low DO, respectively, the unidentified product may have formed by species that would otherwise decompose to NO_3^-, potentially limiting the UF+RNS model (rev. 1) to assess DBP formation until it is incorporated into the model. At pH 9, reactions 1−6 from Kirsch et al.[16] were identified as major contributors to NO_3^- formation.

$$ONOOH \rightarrow HNO_3 \quad (1)$$

$$ONOOH \rightarrow NO_2^{\bullet} + HO^{\bullet} \quad (2)$$

$$2NO_2^{\bullet} \rightarrow N_2O_4 \quad (3)$$

$$N_2O_4 + H_2O \rightarrow HNO_3 + HNO_2 \quad (4)$$

$$ONOOH + H_3O^+ \rightarrow NO_2^+ + 2H_2O \quad (5)$$

$$NO_2^+ + 2H_2O \rightarrow HNO_3 + H_3O^+ \quad (6)$$

The unidentified product may form by the N-containing reactants in these reactions (i.e., ONOOH, $NO_2^{\bullet}$, N_2O_4, or NO_2^+) and chlorine-containing species from the chloramine system like HOCl, NH_2Cl, and $NHCl_2$. Because the unidentified product may comprise about 5−20% of the N mass balance under ambient DO, it could form at $\mu g \cdot L^{-1}$ levels in drinking water systems, like currently regulated DBPs.[46] Revealing the structure of the unidentified product and measuring it kinetically during $NHCl_2$ decomposition is needed prior to making further revisions to the UF+RNS model (rev. 1) and is the subject of ongoing research.

■ ASSOCIATED CONTENT

Supporting Information

The Supporting Information is available free of charge at https://pubs.acs.org/doi/10.1021/acs.est.3c08088.

UF and UF+RNS model of chloramine chemistry, reagent preparations, analytical methods and interferences, impact of borate buffer, DO microelectrode correction, corrected UF+RNS model (rev. 1), NDMA formation, $NHCl_2$ decomposition end-products, and N and O mass balances (PDF)

■ AUTHOR INFORMATION

Corresponding Author

Julian L. Fairey − *Department of Civil Engineering, University of Arkansas, Fayetteville, Arkansas 72701, United States;* orcid.org/0000-0003-3129-3929; Email: julianf@uark.edu

Authors

Huong T. Pham − *Department of Civil Engineering, University of Arkansas, Fayetteville, Arkansas 72701, United States*

David G. Wahman − *Drinking Water Treatment and Distribution Branch, Water Infrastructure Division, Center for Environmental Solutions & Emergency Response, U.S. Environmental Protection Agency, Cincinnati, Ohio 45268, United States;* orcid.org/0000-0002-0167-8468

https://doi.org/10.1021/acs.est.3c08088
Environ. Sci. Technol. 2024, 58, 2048−2057

Complete contact information is available at:
https://pubs.acs.org/10.1021/acs.est.3c08088

Notes

The authors declare no competing financial interest.

■ ACKNOWLEDGMENTS

This work was supported by the National Science Foundation Award Number 2034481 and an Arkansas Water Resources Center student grant. The authors acknowledge Matthew Alexander and Levi Haupert (EPA, Cincinnati OH) for helpful comments on a previous draft of this manuscript and Erik Pollock (Stable Isotope Laboratory, University of Arkansas) for help with the nitrogen gas method development. Research was not performed or funded by EPA and was not subject to EPA's quality system requirements. Views expressed are those of the authors and do not necessarily represent views or policies of EPA.

■ REFERENCES

(1) Ratnayaka, D. D.; Brandt, M. J.; Johnson, K. M. Disinfection of Water. In *Water Supply*, 6th ed.; Ratnayaka, D. D.; Brandt, M. J.; Johnson, K. M., Eds.; Butterworth-Heinemann, 2009; Chapter 11, pp 425−461.
(2) Cornwell Engineering Group. *2017 Water Utility Disinfection Survey Report*; American Water Works Association, 2018.
(3) American Water Works Association. *M56: Nitrification Prevention and Control in Drinking Water*: Denver, CO, 2013.
(4) Vikesland, P. J.; Ozekin, K.; Valentine, R. L. Effect of Natural Organic Matter on Monochloramine Decomposition: Pathway Elucidation through the Use of Mass and Redox Balances. *Environ. Sci. Technol.* **1998**, *32* (10), 1409−1416.
(5) Pham, H. T.; Wahman, D. G.; Fairey, J. L. Updated Reaction Pathway for Dichloramine Decomposition: Formation of Reactive Nitrogen Species and *N*-Nitrosodimethylamine. *Environ. Sci. Technol.* **2021**, *55* (3), 1740−1749.
(6) Wei, I. W. In *Chlorine-Ammonia Breakpoint Reactions: Kinetics and Mechanism*; Harvard University: Cambridge, MA, 1972.
(7) Leao, S. F. Kinetics of Combined Chlorine: Reaction of Substitution and Redox. Ph.D. Dissertation, University of California, Berkeley, Berkeley, CA, 1981.
(8) Jafvert, C. T.; Valentine, R. L. Dichloramine Decomposition in the Presence of Excess Ammonia. *Water Res.* **1987**, *21* (8), 967−973.
(9) Jafvert, C. T.; Valentine, R. L. Reaction Scheme for the Chlorination of Ammoniacal Water. *Environ. Sci. Technol.* **1992**, *26* (3), 577−586.
(10) Wahman, D. G. Web-Based Applications to Simulate Drinking Water Inorganic Chloramine Chemistry. *J.—Am. Water Works Assoc.* **2018**, *110* (11), E43−E61.
(11) Jafvert, C. T. A Unified Chlorine-Ammonia Speciation and Fate Model. Ph.D. Dissertation, University of Iowa, 1985.
(12) Shafirovich, V.; Lymar, S. V. Nitroxyl and its Anion in Aqueous Solutions: Spin States, Protic Equilibria, and Reactivities Toward Oxygen and Nitric Oxide. *Proc. Natl. Acad. Sci. U.S.A.* **2002**, *99* (11), 7340−7345.
(13) Doctorovich, F.; Marti, M. A.; Farmer, P. J. In *The Chemistry and Biology of Nitroxyl (HNO)*; Elsevier, 2017.
(14) Wahman, D. G.; Speitel, G. E.; Machavaram, M. V. A Proposed Abiotic Reaction Scheme for Hydroxylamine and Monochloramine under Chloramination Relevant Drinking Water Conditions. *Water Res.* **2014**, *60*, 218−227.
(15) Vikesland, P. J.; Ozekin, K.; Valentine, R. L. Effect of natural organic matter on monochloramine decomposition: Pathway elucidation through the use of mass and redox balances. *Environ. Sci. Technol.* **1998**, *32* (10), 1409−1416.
(16) Kirsch, M.; Korth, H. G.; Wensing, A.; Sustmann, R.; de Groot, H. Product Formation and Kinetic Simulations in the pH Range 1−14 Account for a Free-Radical Mechanism of Peroxynitrite Decomposition. *Arch. Biochem. Biophys.* **2003**, *418* (2), 133−150.
(17) Schreiber, I. M.; Mitch, W. A. Nitrosamine Formation Pathway Revisited: The Importance of Chloramine Speciation and Dissolved Oxygen. *Environ. Sci. Technol.* **2006**, *40* (19), 6007−6014.
(18) Choi, J.; Valentine, R. L. Formation of N-nitrosodimethylamine (NDMA) from reaction of monochloramine: A new disinfection by-product. *Water Res.* **2002**, *36* (4), 817−824.
(19) Richardson, S. D.; Plewa, M. J.; Wagner, E. D.; Schoeny, R.; DeMarini, D. M. Occurrence, genotoxicity, and carcinogenicity of regulated and emerging disinfection by-products in drinking water: A review and roadmap for research. *Mutat. Res., Rev. Mutat. Res.* **2007**, *636* (1−3), 178−242.
(20) Uppu, R. M.; Squadrito, G. L.; Bolzan, R. M.; Pryor, W. A. Nitration and Nitrosation by Peroxynitrite: Role of CO2 and Evidence for Common Intermediates. *J. Am. Chem. Soc.* **2000**, *122* (29), 6911−6916.
(21) Leung, S. W.; Valentine, R. L. An Unidentified Chloramine Decomposition Product-I. Chemistry and Characteristics. *Water Res.* **1994**, *28* (6), 1475−1483.
(22) Valentine, R. L.; Brandt, K. I.; Jafvert, C. T. A Spectrophotometric Study of the Formation of an Unidentified Monochloramine Decomposition Product. *Water Res.* **1986**, *20* (8), 1067−1074.
(23) Valentine, R. L.; Wilber, G. G. Some Physical and Chemical Charactersitics of an Unidentified Product of Inorganic Chloramine Decomposition. In *Water Chlorination: Chemistry, Enviromental Impact and Health Effects*; Jolley, R. L., Ed.; Lewis, 1990; pp 819−832.
(24) Hand, V. C. Kinetics and Mechanisms of the Decomposition of N-Chloro-alpha-Amino Acids and Dichloramine in Aqueous Solutions. Ph.D. Dissertation, Purdue University, Ann Arbor, 1982.
(25) Cao, Z.; Yu, X.; Zheng, Y.; Aghdam, E.; Sun, B.; Song, M.; Wang, A.; Han, J.; Zhang, J. Micropollutant abatement by the UV/chloramine process in potable water reuse: A review. *J. Hazard. Mater.* **2022**, *424*, 127341.
(26) Huang, L.; Li, L.; Dong, W.; Liu, Y.; Hou, H. Removal of Ammonia by OH Radical in Aqueous Phase. *Environ. Sci. Technol.* **2008**, *42* (21), 8070−8075.
(27) Hoigne, J.; Bader, H. Ozonation of water: kinetics of oxidation of ammonia by ozone and hydroxyl radicals. *Environ. Sci. Technol.* **1978**, *12* (1), 79−84.
(28) Hooper, D. C.; Scott, G. S.; Zborek, A.; Mikheeva, T.; Kean, R. B.; Koprowski, H.; Spitsin, S. V. Uric acid, a peroxynitrite scavenger, inhibits CNS inflammation, blood-CNS barrier permeability changes, and tissue damage in a mouse model of multiple sclerosis. *FASEB J.* **2000**, *14* (5), 691−698.
(29) Hooper, D. C.; Spitsin, S.; Kean, R. B.; Champion, J. M.; Dickson, G. M.; Chaudhry, I.; Koprowski, H. Uric acid, a natural scavenger of peroxynitrite, in experimental allergic encephalomyelitis and multiple sclerosis. *Proc. Natl. Acad. Sci. U.S.A.* **1998**, *95* (2), 675−680.
(30) Kean, R. B.; Spitsin, S. V.; Mikheeva, T.; Scott, G. S.; Hooper, D. C. The Peroxynitrite Scavenger Uric Acid Prevents Inflammatory Cell Invasion into the Central Nervous System in Experimental Allergic Encephalomyelitis through Maintenance of Blood-Central Nervous System Barrier Integrity. *J. Immunol.* **2000**, *165* (11), 6511−6518.
(31) Benjamin, M. M. *Water Chemistry*; McGraw-Hill, 2002.
(32) Reichert, P. AQUASIM - A tool for simulation and data analysis of aquatic systems. *Water Sci. Technol.* **1994**, *30* (2), 21−30.
(33) Yang, L.; Chen, Z. L.; Shen, J. M.; Xu, Z. Z.; Liang, H.; Tian, J. Y.; Ben, Y.; Zhai, X.; Shi, W. X.; Li, G. B. Reinvestigation of the Nitrosamine-Formation Mechanism during Ozonation. *Environ. Sci. Technol.* **2009**, *43* (14), 5481−5487.
(34) Valentine, R. L.; Jafvert, C. T. General acid catalysis of monochloramine disproportionation. *Environ. Sci. Technol.* **1988**, *22* (6), 691−696.
(35) Gerasimov, O. V.; Lymar, S. V. The Yield of Hydroxyl Radical from the Decomposition of Peroxynitrous Acid. *Inorg. Chem.* **1999**, *38* (19), 4317−4321.

(36) Hodges, G. R.; Ingold, K. U. Cage-Escape of Geminate Radical Pairs Can Produce Peroxynitrate from Peroxynitrite under a Wide Variety of Experimental Conditions1. *J. Am. Chem. Soc.* **1999**, *121* (46), 10695−10701.
(37) Beckman, J. S.; Beckman, T. W.; Chen, J.; Marshall, P. A.; Freeman, B. A. Apparent hydroxyl radical production by peroxynitrite: implications for endothelial injury from nitric oxide and superoxide. *Proc. Natl. Acad. Sci. U.S.A.* **1990**, *87* (4), 1620−1624.
(38) Lymar, S. V.; Hurst, J. K. Rapid Reaction between Peroxonitrite Ion and Carbon Dioxide: Implications for Biological Activity. *J. Am. Chem. Soc.* **1995**, *117* (34), 8867−8868.
(39) Squadrito, G. L.; Pryor, W. A. Mapping the reaction of peroxynitrite with CO_2: Energetics, reactive species, and biological implications. *Chem. Res. Toxicol.* **2002**, *15* (7), 885−895.
(40) Smulik, R.; Debski, D.; Zielonka, J.; Michalowski, B.; Adamus, J.; Marcinek, A.; Kalyanaraman, B.; Sikora, A. Nitroxyl (HNO) Reacts with Molecular Oxygen and Forms Peroxynitrite at Physiological pH: Biological Implications. *J. Biol. Chem.* **2014**, *289* (51), 35570−35581.
(41) Sharpless, C. M.; Linden, K. G. UV Photolysis of Nitrate: Effects of Natural Organic Matter and Dissolved Inorganic Carbon and Implications for UV Water Disinfection. *Environ. Sci. Technol.* **2001**, *35* (14), 2949−2955.
(42) Do, T. D.; Pifer, A. D.; Wahman, D. G.; Hickman, R. N.; Chimka, J. R.; Fairey, J. L. Nitrite Quantification by Second Derivative Chemometric Models Mitigates Natural Organic Matter Interferences under Chloraminated Drinking Water Distribution System Conditions. *Water Res.* **2023**, *229* (2), 119430.
(43) Schreiber, I. M.; Mitch, W. A. Influence of the Order of Reagent Addition on NDMA Formation During Chloramination. *Environ. Sci. Technol.* **2005**, *39* (10), 3811−3818.
(44) Olagunju, O. M. Peroxynitrite Chemistry: Formation, Decomposition and Possible Deactivation Mechanisms by Thiols. Ph.D. Dissertation, Portland State University, 2008.
(45) Pryor, W. A.; Squadrito, G. L. The Chemistry of Peroxynitrite: A Product from the Reaction of Nitric Oxide and Superoxide. *Am. J. Physiol.: Lung Cell. Mol. Physiol.* **1995**, *268* (5), L699−L722.
(46) Arora, H.; LeChevallier, M. W.; Dixon, K. L. DBP occurrence survey. *J. - Am. Water Works Assoc.* **1997**, *89* (6), 60−68.

https://doi.org/10.1021/acs.est.3c08088
Environ. Sci. Technol. 2024, 58, 2048−2057